(8) Krigas, T. M.; Carella, J. M.; Struglinski, M. J.; Crist, B.; Graessley, W. W. *J. Polym. Sci., Poly. Phys. Ed.* **1985**, *23*, 509.
(9) Graessley, W. W., private communication.
(10) Jackson, J. F. *J. Polym. Sci., Part A* **1963**, *I*, 2119.
(11) Burfield, D. R. *Makromol. Chem.* **1985**, *186*, 2657.
(12) Ham, G. E. *Copolymerization*; Interscience: New York, 1964; Vol. XVIII, Chapter I.
(13) Usami, T.; Gotoh, Y.; Takayama, S. *Macromolecules* **1986**, *19*, 2722.
(14) Natta, G.; Mazzanti, G.; Valvassori, A.; Sartori, G.; Morero, D. *Chim. Ind. (Milan)* **1960**, *42*, 125.
(15) Killian, H. G. *Kolloid-Z.* **1963**, *189*, 23.
(16) Kakugo, M.; Naito, Y.; Mizunuma, K.; Miyatake, T. *Macromolecules* **1982**, *15*, 1150.

# Characterization of a Polymer Blend by the Spin Label Method: Concentration of Poly(methyl methacrylate) in a Blend with Poly(vinylidene fluoride)

**Shigetaka Shimada,* Yasurō Hori, and Hisatsugu Kashiwabara**

*Nagoya Institute of Technology, Gokiso-cho, Nagoya 466, Japan.*
*Received September 30, 1987; Revised Manuscript Received May 18, 1988*

ABSTRACT: The electron spin resonance line shape of nitroxide radical labels attached to poly(methyl methacrylate) (PMMA) side chains in blends with poly(vinylidene fluoride) (PVDF) was studied as a function of PVDF content. The principal values are anisotropic hyperfine splitting ($A_{Z'}$) due to the nitrogen nucleus and the line width increase with PVDF content. The increase, $\Delta A_{Z'}$, can be attributed to the effect of the electric field of a PVDF chain in a molecularly compatible system. The outermost splitting width ($2A_Z$) observed at −196 °C was a good measure of PMMA concentration in the molecularly mixed phase. Estimation of the concentrations of both phases in a phase-separated system as a function of annealing temperature indicated that an upper critical solution temperature (UCST) exists at about 100 °C.

## Introduction

Many authors have studied blends of poly(methyl methacrylate) (PMMA) and poly(vinylidene fluoride) (PVDF).[1] The general conclusion is that these components are compatible in an amorphous state, i.e., above the melting point of PVDF ($T_m \simeq 170$ °C). Below $T_m$, the PVDF chain crystallizes from a molten blend, especially at high PVDF content. Bernstein et al.[1b] and Hirata and Kotaka[1c] observed lower critical solution temperature behavior at temperatures above 200 °C. On the other hand, Saito et al.[1i] concluded that phase separation takes place at an upper critical solution temperature (UCST) around 100 °C, based on the crystallization of PVDF from the melt at various temperatures. Hahn et al.[1j] also concluded that the amorphous PVDF interphase separates from crystalline and mixed amorphous regions. Blends of PMMA and PVDF are generally composed of a crystalline phase of PVDF and a liquidlike amorphous phase; the amorphous phase may be composed of PMMA-rich and PVDF-rich phases in a phase-separated system.

Since it is not certain that the amorphous region is completely phase-separated, it is important to estimate unambiguously the concentration of the respective chains in both phases. The ESR method is a simple and effective way of determining the molecular structure and molecular motion of only one kind of a spin-labeled polymer chain in a complicated system.[2]

Our aim in this study was to determine the concentration of spin-labeled PMMA in a PMMA/PVDF blend and to assess the translational diffusion of PMMA chains in relation to the molecular compatibility of the components.

## Experimental Section

**Materials.** PVDF was Kynar 731 powder (Pennwalt Chemical Co., Ltd.). Spin-labeled PMMA was prepared by anionic copolymerization of MMA monomer (Tokyo Kasei Co., Ltd.) with a labeled monomer, 4-(methacryloyloxy)-2,2,6,6-tetramethylpiperidine,[3] using butyllithium catalyst at −78 °C. The mole ratio of labeled monomer to MMA monomer was less than 1:250. The weight-average molecular weight, $M_w$, and the number-average molecular weight, $M_n$, are, respectively, 462 000 and 80 800 for PVDF and 125 000 and 29 000 for PMMA. The tacticity of the PMMA, determined by high-resolution $^1$H NMR,[4] was isotactic 88%, heterotactic 4%, and syndiotactic 8% in terms of triads. Another probe, 4-hydroxy-2,2,6,6-tetramethylpiperidine-1-oxyl (TANOL) was also used to confirm the intermolecular interaction between nitroxide radicals and polymer chains.

**Preparation of Blends.** Blends were made by mixing spin-labeled PMMA and PVDF in the ratios 70:30, 50:50, 33:67, and 11:89 by weight. Films of blends and of spin-labeled PMMA were prepared by casting from ~3 wt % acetone solution at 50 °C. The films were dried under vacuum for more than 1 day at room temperature. Films of spin-probed PMMA and spin-probed PVDF (~$6 \times 10^{-4}$ mol of Tanol per mole of polymer) were prepared by the same method.

**ESR Measurements.** Samples were stacked in ESR sample tubes evacuated to $10^{-5}$ mmHg. ESR measurements were carried out with a JEOL FE3XG spectrometer with a connected MELCOM 70/25 computer. The signal of diphenylpicrylhydrazyl (DPPH) was used as a $g$-value standard. The magnetic field sweep was calibrated with the known splitting constant of $Mn^{2+}$.

**Simulation.** Computer simulation was carried out in order to obtain the principal values of $g$ and $A$ tensors and the line width. Since it was reasonable to assume that the nitroxide radicals have a completely random orientation, the $g$ and $A$ values could be computed from eq 1 and 2,[5] choosing the 8100 sets of

$$g = (g_{X'}^2 \sin^2\theta \sin^2\phi + g_{Y'}^2 \sin^2\theta \cos^2\phi + g_{Z'}^2 \cos^2\theta) \quad (1)$$

$$A = (g_{X'}^2 A_{X'}^2 \sin^2\phi + g_{Y'}^2 A_{Y'}^2 \sin^2\theta \cos^2\phi + g_{Z'}^2 A_{Z'}^2 \cos^2\theta)^{1/2} \quad (2)$$

$(\theta, \phi)$ in a solid angle of $\pi/2$, where $g_{X'}$, $g_{Y'}$, and $g_{Z'}$, are the principal values of the $g$ tensor and $A_{X'}$, $A_{Y'}$, and $A_{Z'}$ are those of the $A$ tensor due to the nitrogen nucleus. It was also assumed that the principal directions of the $g$ and $A$ tensors coincided. Several theoretical spectra were calculated by gradually changing the principal values and the line width of the Gaussian line shape function. These spectra were recorded on an $X$–$Y$ plotter and

0024-9297/88/2221-3454$01.50/0 

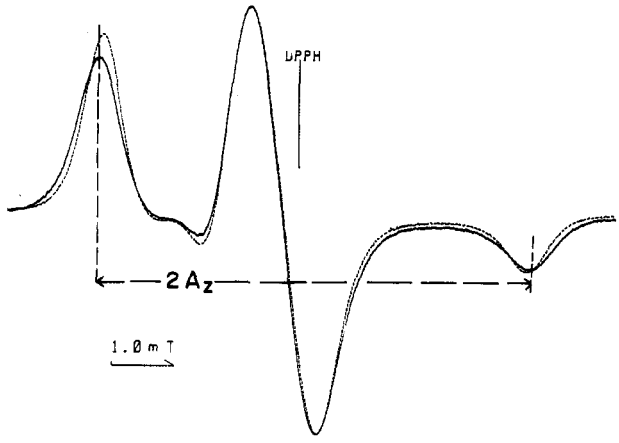


**Figure 1.** ESR spectra of nitroxide radical labels on PMMA chains in PMMA (dotted line) and in a 33/67 blend (solid line). The vertical dotted line is the spectrum of DPPH, $g = 2.0036$.

**Table I**
**ESR Parameters of Spin Probe and Spin Label in PMMA and PMMA/PVDF Blends, Obtained by Spectral Simulation**

| | probe | | label | |
|---|---|---|---|---|
| | TANOL/ PMMA | TANOL/ PVDF | PMMA-L/ PMMA | PMMA-L/ PMMA–PVDF (33/67) |
| $g_{x'}$ | 2.0020 | 2.0022 | 2.0020 | 2.0021 |
| $g_{y'}$ | 2.0064 | 2.0064 | 2.0064 | 2.0067 |
| $g_{z'}$ | 2.0098 | 2.0093 | 2.0096 | 2.0091 |
| $g_i$ | 2.0061 | 2.0060 | 2.0060 | 2.0060 |
| $A_{x'}$, mT | 3.42 | 3.50 | 3.39 | 3.44 |
| $A_{y'}$, mT | 0.64 | 0.63 | 0.60 | 0.62 |
| $A_{z'}$, mT | 0.68 | 0.69 | 0.70 | 0.66 |
| $A_i$, mT | 1.58 | 1.61 | 1.56 | 1.57 |
| $\Delta H'$, mT | 0.65 | 0.79 | 0.71 | 0.82 |

compared with the observed spectra in order to get the best fit.

## Results and Discussion

**ESR Spectra of Nitroxide Radical Labels.** In order to observe ESR spectra of nitroxide labels on PMMA chains in completely compatible blends, the samples were melted at 190 °C for 15 min and then plunged into liquid nitrogen. The ESR measurements were carried out at −196 °C.

Figure 1 shows the ESR spectrum of nitroxide radicals on PMMA compared with that of the 33/67 blend. The width between the outermost peaks ($2A_Z$) and the line width ($\Delta H'$) of the spectrum of the 33/67 blend is larger than those in PMMA. The outermost splitting widths of the main triplet spectra are due to hyperfine coupling caused by the nitrogen nucleus ($A_{Z'}$). These results mean that the nitroxide radicals are affected by the environment of the radical sites, for example, the states of aggregation in molecularly compatible regions in the blends. In order to confirm these effects, ESR spectra of spin-probed PMMA and spin-probed PVDF were compared. The values of $2A_Z$ and $\Delta H'$ in PVDF matrices are larger than those in PMMA as indicated by the spin-labeled polymers. Simulated spectra agreed well with the experimental spectra. The ESR parameters of the radicals in the PMMA-rich and PVDF-rich matrices are given in Table I.

The values of $A_{Z'}$ and $\Delta H'$ for the radicals in the PVDF-rich matrices are larger than those in the PMMA matrices although the principal value of $g_X$ in PVDF is smaller than that in PMMA. Griffith et al. showed that there is a small solvent effect on the ESR spectra of nitroxide spin labels and developed a semiquantitative

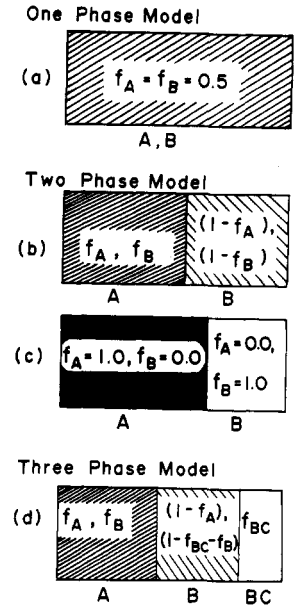


**Figure 2.** Two-phase and three-phase models of a binary mixture of polymers A and B, where $f_A$ and $f_B$ are mole fractions of the respective polymers and $f_{BC}$ is the degree of crystallinity in polymer B.

treatment of this effect.[6] The variations of $A_{Z'}$ and $\Delta H'$ observed in our study should arise from the electric field of the polar groups as concluded by Griffith et al. The solvent dependence of ESR spectra can be visualized as arising from changes in the relative contributions of the two canonical structures A and B of the neutral nitroxide free radical. The changes are caused by the electric field

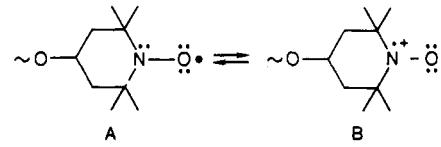


of the PVDF chain. Structure A localizes the unpaired electron on the oxygen atom, whereas structure B localizes it on the nitrogen atom, and the electric field that tends to stabilize B is responsible for the increasing hyperfine splitting due to the nitrogen nucleus.

The increase of $\Delta H'$ in the PVDF-rich matrices may be caused by the increase of a distribution of the intermolecular interactions between the radical and the polymer chain. The overall effects of the intermolecular interaction on the ESR parameters $A_{Z'}$ and $\Delta H'$ should be represented as the outermost splitting ($2A_Z$), which we found to be proportional to the mole fraction of PVDF. This fact suggests that the spin-labeled PMMA is molecularly and uniformly mixed with PVDF in a compatible blend and that $2A_Z$ is a good measure of the concentration of PMMA chains in the mixed system.

**Estimation of the Concentration of PMMA Chains in a Mixed Phase of a Blend.** We estimated the concentration of PMMA chains in a mixed phase by using the proportionality of $2A_Z$ to the mole fraction of PVDF ($C_B$) in the blend:

$$2A_Z - 2A_0 = KC_B = K\frac{N_B}{N_A + N_B} = K\frac{r}{1+r} \qquad r = \frac{N_B}{N_A} \tag{3}$$

where $2A_0$ is the outermost separation in the spectrum of PMMA, $N_A$ and $N_B$ are mole fractions of A and B polymers, and $K$ is a constant.

**Two-Phase Model.** We denote by $f_A$ and $f_B$ the fractions of monomer units of PMMA and PVDF, respectively,

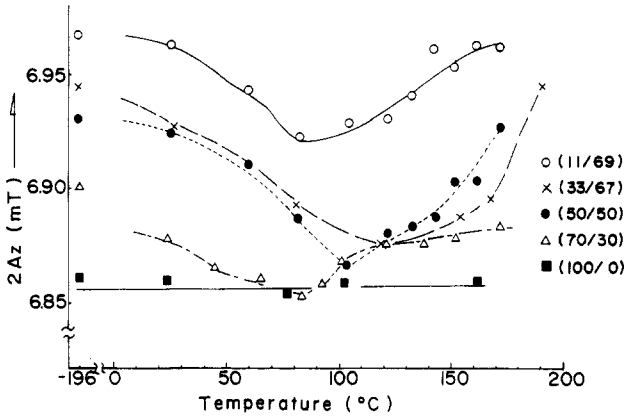


**Figure 3.** Outermost separation ($2A_Z$) of the ESR spectrum of nitroxide radicals versus annealing temperature in a quenched blend.

in the PMMA-rich phase of a phase-separated blend. The fractions of the monomer units of PMMA and PVDF in the PVDF-rich phase are then $1 - f_A$ and $1 - f_B$, respectively (Figure 2b). Thus, $f_A = f_B = 0.5$ represents a completely compatible blend (Figure 2a), whereas $f_A = 1.0$, $f_B = 0$ in the PMMA-rich phase represents a completely separated phase (Figure 2c). The average concentration of A (PMMA) polymer ($C_A$) is represented by

$$C_A = (1 - C_B) = C_{AA}f_A + C_{AB}(1 - f_A) \tag{4}$$

where $C_{AA}$ and $C_{AB}$ are the mole concentrations of the A chain in the A-rich and the B-rich phases, respectively:

$$C_{AA} = \frac{f_A N_A}{f_A N_A + f_B N_B} = \frac{f_A}{f_A + f_B r} \tag{5}$$

$$C_{AB} = \frac{1 - f_A}{(1 - f_A) + (1 - f_B)r} \tag{6}$$

Equations 3–6 lead to eq 7:

$$X = 1 - \frac{2A_Z - 2A_0}{K} = \frac{f_A^2}{f_A + f_B r} + \frac{(1 - f_A)^2}{(1 - f_A) + (1 - f_B)r} \tag{7}$$

The values of $X$ can be calculated for the values of $f_A$ and $f_B$, which are in the ranges of 0.5–1.0 and 0.5–0, respectively. From plots of $X$ versus $f_A$ versus and the experimental values of $X$, the values $f_A$ and $f_B$ can be determined, although the values have some uncertainty. The concentrations $C_{AA}$ and $C_{AB}$ can then be calculated from eq 5 and 6. The mole fractions of the total polymers in both PMMA-rich ($M_A$) and PVDF-rich ($M_B$) phases can be calculated from

$$M_A = \frac{f_A N_A + f_B N_B}{N_A + N_B} = \frac{f_A + f_B r}{1 + r} \tag{8}$$

$$M_B = \frac{(1 - f_A)N_A + (1 - f_B)N_B}{N_A + N_B} = \frac{(1 - f_A) + (1 - f_B)r}{1 + r} \tag{9}$$

**Three-Phase Model.** When PVDF (B) polymers crystallize during annealing at high temperatures, one can consider a three-phase model (Figure 2d). The concentrations, $C_{AA}$ and $C_{AB}$, can be represented by

$$C_{AA} = \frac{f_A}{f_A + f_B r} \tag{10}$$

$$C_{AB} = \frac{1 - f_A}{(1 - f_A) + (1 - f_{BC} - f_B)r} \tag{11}$$

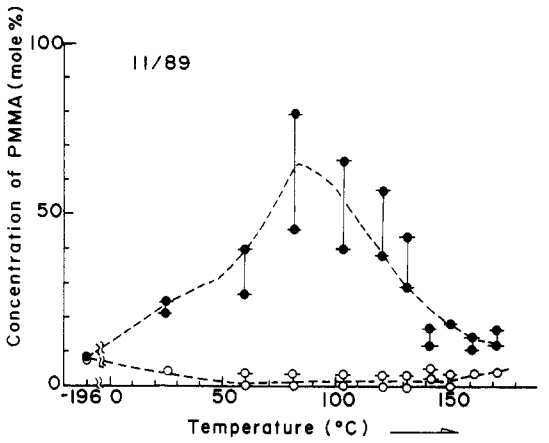


**Figure 4.** Concentrations of PMMA chains versus annealing temperature in PMMA-rich (●) and PVDF-rich (○) phases in a 11/89 blend.

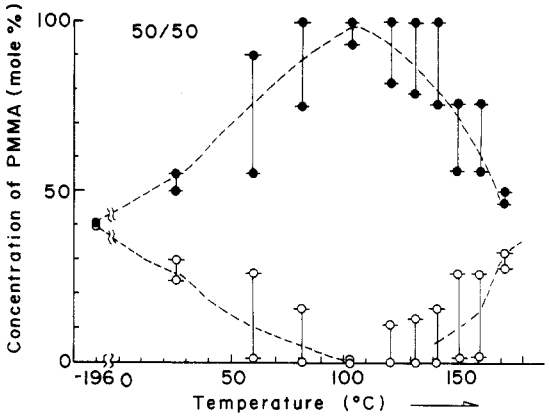


**Figure 5.** Concentrations of PMMA chains versus annealing temperature in PMMA-rich (●) and PVDF-rich (○) phases in a 50/50 blend.

where $f_{BC}$ is the degree of crystallinity in the B polymer. The value of $X$ can be represented by

$$X = \frac{f_A^2}{f_A + f_B r} + \frac{(1 - f_A)^2}{(1 - f_A) + (1 - f_{BC} - f_B)r} \tag{12}$$

The first term on the right side is in general much larger than the second term. Therefore, the estimate of $C_{AA}$ is almost the same as that from the two-phase model. On the other hand, the value of $C_{AB}$ is estimated to be a little larger than that in the two-phase model even for $f_{BC} = 0.5$.

**Change of Concentration of PMMA Chains in Mixed Phases of Blends.** In Figure 3, the outermost separations are plotted against annealing temperature. The value of $2A_Z$ is constant for PMMA. However, in the blends, $2A_Z$ has a minimum value around 100 °C, indicating that the average concentration of PMMA chains in the mixed phases has a maximum value at about the same temperature. Thus, a phase separation occurs in the lower temperature range, and molecular mixing occurs in the higher temperature range.

In order to confirm this result, we calculated the concentration of PMMA chains, $C_{AA}$ and $C_{AB}$, in the mixed phases for the two-phase model by the method mentioned in the previous section. In Figures 4 and 5 are shown plots of $C_{AA}$ and $C_{AB}$ against annealing temperature for the 11/89 and 50/50 blends. The concentration $C_{AA}$ in the PMMA-rich phase increases and the concentration $C_{AB}$ in the PVDF-rich phase decreases with increasing temperature in the lower temperature range. On the other hand, $C_{AA}$ decreases and $C_{AB}$ increases in the higher temperature range. The concentrations, $C_{AA}$ and $C_{AB}$, in the 50/50

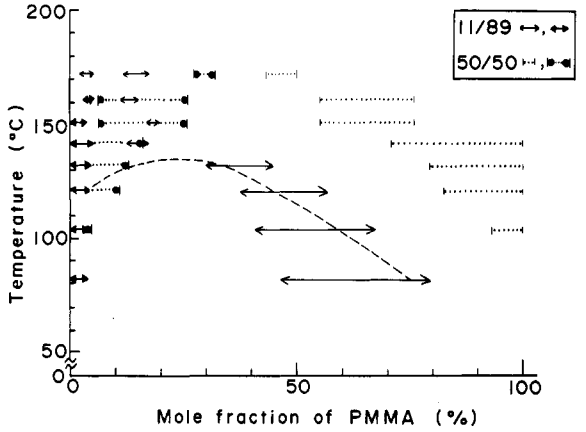


**Figure 6.** Concentrations of PMMA chains in mixed phases. Phase, PVDF rich, PMMA rich; 11/89, ↔, ↔; 50/50, |●···●|, |···|. Dashed line is phase diagram of PMMA/PVDF based on ref 1i.

blend were 0.93–1.00 and 0–0.05, respectively, at 104 °C, indicating that the annealed blend is composed of almost pure PMMA and PVDF phases. Thus, almost complete separation into individual polymer phases takes place during annealing at 104 °C.

These facts provide a compelling argument that phase separation occurs in the lower temperature range and that molecular mixing occurs in the higher temperature range by translational molecular diffusion of PMMA and PVDF chains. The mole fractions of the polymers in both phases can be estimated from eq 8 and 9. The changes in the mole fractions are similar to those of the concentrations, $C_{AA}$ and $C_{AB}$, shown in Figures 4 and 5. For example, the fractions in the PMMA-rich and the PVDF-rich phases have minimum (0.05–0.16) and maximum (0.84–0.95) values, respectively, at 82 °C in the 11/89 blend.

**Upper Critical Solution Temperature of the Blend.** If the concentrations in the mixed phases estimated in the previous section are in thermodynamic equilibrium, it should be possible to obtain a phase diagram of PMMA/PVDF. In Figure 6 are plotted the mole concentrations of PMMA chains in two mixed phases against annealing temperature for the 11/89 and 50/50 blends. The phase diagram is based on literature data.[1i] The concentrations calculated from the data for the 11/89 blend agree well with the results of Saito et al.[1i] On the other hand, those from the data for the 50/50 blend deviate from these results. This result may mean that translational molecular diffusion is slower in the 50/50 blend and that achievement of an equilibrium compatible state is more difficult than in the 11/89 blend. It has been reported[2] that the rotational and translational molecular motions of PMMA chains become rapid with increasing content of PVDF in a compatible blend. The changes of the concentrations in the mixed phases shown in Figure 6 indicate the existence of an upper critical solution temperature (UCST) at about 100 °C and support the conclusion of Saito et al.[1i]

**Registry No.** PMMA, 9011-14-7; PVDF, 24937-79-9; TANOL, 2226-96-2; (MMA)(4-methacryloyloxy)-2,2,6,6-tetramethylpiperidine) (copolymer), 70800-02-1.

## References and Notes

(1) For example: (a) Nishi, T.; Wang, T. T. *Macromolecules* **1975**, *8*, 909. (b) Bernstein, R. E.; Cruz, C. A.; Paul, D. R.; Barlow, J. W. *Macromolecules* **1977**, *10*, 681. (c) Hirata, Y.; Kotaka, T. *Polym. J. (Tokyo)* **1981**, *13*, 273. (d) Wendorff, J. H. *J. Polym. Sci., Polym. Lett. Ed.* **1980**, *18*, 439. (e) Bliznyuk, V. N.; Shilov, V. V.; Gomza, Yu. P.; Lipatov, Yu. S. *Polym. Sci. USSR (Engl. Transl.)* **1985**, *77*, 147. (f) Hahn, B. R.; Wendorff, J. H.; Yoon, D. Y. *Macromolecules* **1985**, *18*, 718. (g) Pathmanathan, K.; Johari, G. P.; Faivre, J. P.; Monnerie, L. *J. Polym. Sci., Polym. Phys. Ed.* **1986**, *24*, 1587. (h) Hahn, B. R.; Wendorff, J. H. *Polymer* **1985**, *26*, 1619. (i) Saito, H.; Fujita, Y.; Inoue, T. *Polym. J. (Tokyo)* **1987**, *19*, 405. (j) Hahn, B. R.; Hermann-Schnherr, O.; Wendorff, J. H. *Polymer* **1987**, *28*, 201.

(2) Shimada, S.; Hori, Y.; Kashiwabara, H. *Polym. Repr. Jpn.* **1986**, *35*, 880.

(3) Ito, I.; Ohnishi, S. Presented at the 9th ESR Symposium, Chemical Society Japan, 1970.

(4) Frisch, H. L.; Mallows, C. L.; Heatley, F.; Bovey, F. A. *Macromolecules* **1968**, *1*, 533.

(5) Gordy, W. *Theory and Applications of Electron Spin Resonance*; Wiley: New York, 1980; p 373.

(6) Griffith, O. H.; Dehlinger, P. J.; Van, S. P. *J. Membr. Biol.* **1974**, *15*, 159.